

Numerical simulation of giant magnetoresistance in magnetic multilayers and granular films

Y. Yamagishi, S. Honda, and J. Inoue*

Department of Applied Physics, Nagoya University, Nagoya 464-8603, Japan

H. Itoh

Department of Pure and Applied Physics, Kansai University, Suita 564-8680, Japan

(Received 20 October 2009; revised manuscript received 8 February 2010; published 26 February 2010)

We perform numerical simulations of conductance and conductivity for magnetic multilayers and magnetic granular films which show giant magnetoresistance (GMR). The system size to which the recursive Green's function method is applied is sufficiently large to eliminate incidental effects caused by the system boundary reported previously. It is shown that the resistivity change in the magnetic granular films is proportional to the inverse of the grain size.

DOI: [10.1103/PhysRevB.81.054445](https://doi.org/10.1103/PhysRevB.81.054445)

PACS number(s): 73.50.-h, 73.61.At, 73.21.Ac

In the two decades after the discovery of giant magnetoresistance (GMR),^{1,2} the field of spintronics has matured, producing applications such as magnetoresistive sensors and memories. The basic physics of GMR is now well understood, thanks to the enormous number of experimental and theoretical studies conducted thus far. Spin dependent scattering is the most crucial concept to understand GMR effects.³⁻⁹ GMR has been observed not only in magnetic multilayers (MMLs) but also in magnetic granular films (MGFs).¹⁰⁻¹⁵

Among the many theoretical studies in this arena, a Boltzmann type semiclassical approach¹⁶ and a quantum approach are the main frameworks to study GMR. The latter theory of transport has been found to be extremely useful and has been frequently applied to MMLs.¹⁷⁻²⁴ There have been only a few cases of application of this theory to MGFs, however, since the translational invariance is completely lost in MGFs, and a real space calculation with a large system size is required. In the early stages of such real space quantum simulations of the conductance, the system size is too small to eliminate incidental effects caused by the boundaries of the system.^{19,20} An additional resistance produced at the contact between the GMR system (sample) and a lead may obscure the numerical results caused by the true GMR effect. Furthermore, the sizes of the magnetic grains in MGFs are not sufficiently large to reproduce the experimental tendency. In spite of these shortcomings, the quantum simulation has been able to grasp the essential features of GMR, for example, it adequately reproduces the difference between CIP(current in plane)-GMR and CPP(current perpendicular to plane)-GMR.^{19,20} Nevertheless, quantitative numerical simulations of GMR for larger system sizes are desirable to eliminate these shortcomings and ensure the derived results.

In this paper, we present results of numerical simulations of the conductance and magnetoresistance (MR) for MMLs and MGFs with a sufficiently large system size. The results of MR for MGFs is examined in detail and compared with experimental results which show a well-defined GMR effect.^{11,13,14}

We adopted a single orbital tight-binding (TB) model with a nearest neighbor hopping integral $-t$, and applied the recursive Green's function method to calculate the conductance Γ for finite size MMLs and MGFs. The system consists

of a sample region, which is either a MML or MGF with two (left and right) leads attached to the sample. Figure 1 shows the structures of the samples for which Γ and MR were calculated; MMLs for CIP- and CPP-geometries, as well as MGFs. The lattice structure is a simple cubic lattice with lattice constant a . The cross section and sample length are $S=40 \times 40$ and $L=400 \sim 3000$ in units of a , respectively. The sample size used in this work is much larger than that ($12 \times 12 \times 12$) used in our previous study.^{19,20}

In experiments, the samples used to measure the CIP-GMR and granular type GMR were sufficiently large, and the electrical resistivity ρ instead of resistance ($1/\Gamma$) was measured. In order to estimate ρ from the calculations of Γ , we used a scaling relation,

$$\frac{1}{\Gamma} = \frac{1}{\Gamma_C} + \rho \frac{L}{S}, \quad (1)$$

where $1/\Gamma_C$ is contact resistance. The resistivity was estimated from the Γ - L relation for sufficiently large values of L . In the case of CPP-GMR, since the samples used in experiments were rather small, we calculated the conductance itself.

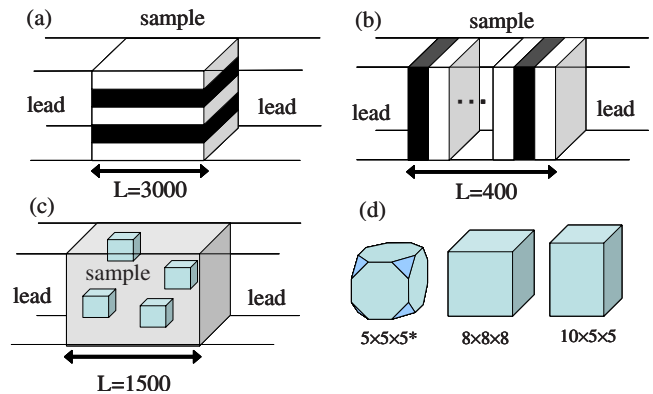


FIG. 1. (Color online) Structures used in the numerical simulations. (a) CIP-GMR system, (b) CPP-GMR system, (c) granular film, and (d) types of grains embedded in (c). The cross section is 40×40 in units of the lattice constant. An asterisk in (d) indicates that the edges of a cluster are truncated.

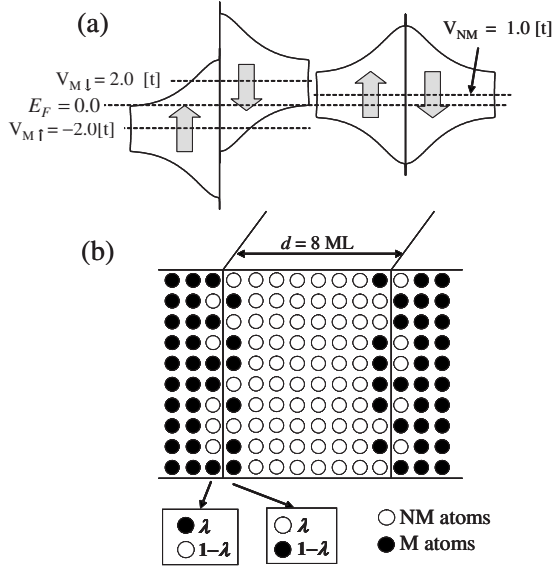


FIG. 2. (a) Densities of states of magnetic and nonmagnetic metals which constitute the magnetic multilayers and granular films. (b) Schematic figures for randomness at the interfaces of magnetic multilayers.

The sample consists of two elements, magnetic (M) and nonmagnetic (NM) metals. We assume that the leads are made of the NM metal. We further assume that the electrical resistivity of the system is given by parallel circuits of up (\uparrow) and down (\downarrow) spin channels (the two-current model). The electronic structure of the \uparrow and \downarrow spin states of the M metal are given by shifting the paramagnetic band of the NM metal. The relative position of the bands of M and NM metals is shown in Fig. 2(a). We assume that the band center of the \uparrow (\downarrow) spin state of the M metal is $2.0t$ lower (higher) than the Fermi energy E_F , and the band center of the NM metal is $1.0t$ higher than E_F . These values correspond to the atomic potentials V_{Ms} and V_{NM} of the M and NM elements, respectively, where $s = \uparrow$ or \downarrow . As can be seen in Fig. 2(a), the band matching between M and NM metals is better in the minority spin state than that in the majority one. We chose this relative position of the bands taking into consideration the electronic structure of the Fe/Cr multilayers. For Co/Cu and Co/Ag multilayers, on the other hand, band matching is better in the majority spin state than that in the minority one. Note, however, that GMR will not depend on whether band matching occurs in the majority or minority spin state. We also use the same parameter values for the MGFs.

Since the interfacial roughness is crucial to GMR, we introduce roughness in such a way that the M and NM atoms at the interfaces are interchanged with a weight λ , as shown in Fig. 2(b).^{19,20} In MGFs, the grains are the source of roughness, and therefore no further roughness is introduced. The shape of the grains used in the simulation is shown in Fig. 1(d). The grains are randomly distributed in the sample. Since the system size is sufficiently large, and self-averaging occurs, we did not prepare many samples with different grain distributions.

Figure 3 shows the calculated results of the MR ratios for MMLs with CIP- and CPP-geometries as functions of λ . The

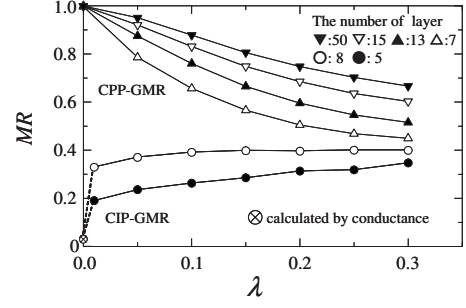


FIG. 3. Calculated results of MR ratios for CIP- and CPP-GMR in magnetic multilayers with different number of layers.

MR ratio for CIP-GMR is defined as $MR = (\rho_{AP} - \rho_P) / \rho_{AP}$ using the resistivity, and that for CPP-GMR is defined as $MR = (\Gamma_P - \Gamma_{AP}) / \Gamma_P$ using the conductance Γ , where P and AP are parallel and antiparallel alignments of the layer magnetization. The resistivity is evaluated using the relation (1). The thickness of the M and NM layers in the CPP-geometry is fixed to be $8a$. The total number of M and NM layers is shown in the figure. In the CIP-geometry, the cross section S is fixed to be 40×40 , and the thickness of the M and NM layers is either $5a$ or $8a$.

The CIP-MR increases with increasing λ . Since band matching of \downarrow spin is good, the \downarrow spin resistivity $\rho_{P\downarrow}$ in P alignment is hardly affected by the replacement of atoms at interfaces. In contrast, the \uparrow spin resistivity $\rho_{P\uparrow}$ is strongly affected by the replacement. Therefore, $\rho_{P\uparrow} / \rho_{P\downarrow}$ increases with increasing λ , resulting in an increase in MR. The CIP-MR for $\lambda = 0$ is obtained from the calculation of the conductance. This value is nonzero, as shown in Figure 3. This is because the change in the magnetization alignment causes a change in the electronic structure of the multilayers, and produces a resistance change.

In contrast to the CIP-GMR, the CPP-MR decreases with increasing λ . Since the MR is caused by band mismatch in the majority spin band, and $\Gamma_{P\downarrow} \gg \Gamma_{P\uparrow}$, MR is high even at $\lambda = 0$ when the sample contains many M and NM layers. Although $\Gamma_{P\downarrow}$ decreases with λ , as in CIP-GMR, $\Gamma_{P\uparrow}$ increases with λ . These results can be explained as follows. When there is no roughness, momentum conservation along layer planes should be satisfied. The restriction is removed by introducing interface roughness, and the conducting paths increase. Since in the \uparrow spin state, the effect is stronger than the roughness which reduces the conductance, $\Gamma_{P\uparrow}$ increases with increasing λ . The results shown in Fig. 3 are essentially the same as those reported previously.^{19,21}

The calculated results of MR and resistivity for MGFs are shown in Figs. 4–6. The MR ratio is defined as $MR = [\rho(0) - \rho(H)] / \rho(0)$, where $\rho(H)$ is the resistivity under an external magnetic field H . It has been assumed that the magnetization direction of grains in the MGFs are distributed randomly at $H = 0$, and align in parallel under a sufficiently high H . The resistivity at a high H will be denoted ρ_P as in GMR in MMLs. The shape of the grains is cubic with a volume r^3 as shown in Fig. 1(d). The parameter values are $V_{M\downarrow} = 2.0t$, $V_{NM} = 1.0t$ and $V_{M\uparrow} = -2.0t$ with 20% concentration of magnetic atoms.

The closed squares in Fig. 4 show the calculated results of

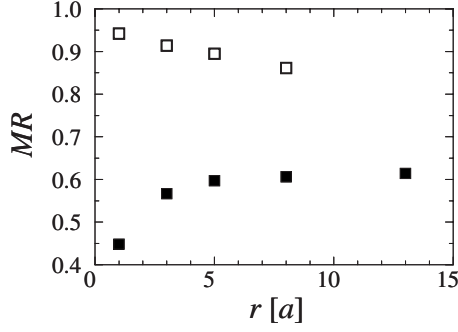


FIG. 4. Calculated results (■) of MR ratios for granular films as functions of grain size r . Results shown by □ are obtained using a different parameter set (see text).

the MR ratio as a function of the grain size r . The MR is nearly independent of the grain size except for the smallest one. The results may be understood by considering the r dependence of $\rho(0)$ and $\rho(H)$ ($\equiv \rho_p$) shown in Fig. 5(a). We see that the linearity of $\rho(0)$ and $\rho(H)$ on $1/r$ holds quite well except for $r=1$. Therefore, MR is nearly independent of r except for small values of r . The dependence of ρ on r can be interpreted as follows.²⁰ Electrons are presumably scattered by surface atoms of magnetic grains. Since the ratio of the number of surface and volume atoms is r^2/r^3 , the resistivity is proportional to $1/r$ for fixed concentration of magnetic atoms.

The results shown by closed squares in Fig. 4 indicate a different tendency from that reported previously.²⁰ The difference may be attributed to parameter values different from

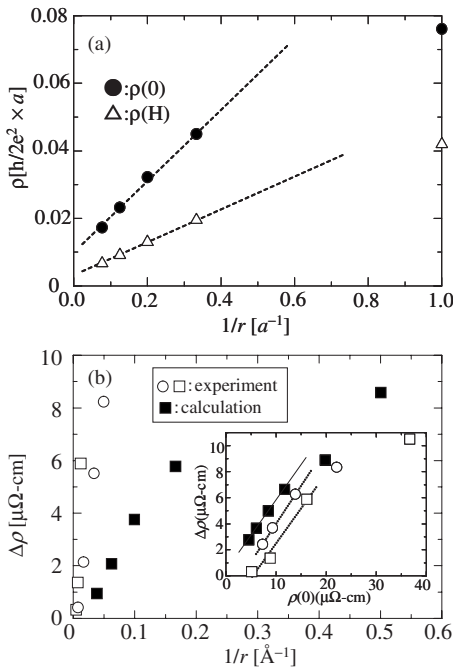


FIG. 5. (a) Calculated results of the resistivity with and without a magnetic field as a function of the inverse of the grain size. (b) Calculated and experimental results (Ref. 13 and 14) of the resistivity change as a function of the inverse of the grain size. The inset shows replots as a function of the resistivity at $H=0$. The parameter values are $V_{M\downarrow}=2.0t$, $V_{NM}=1.0t$ and $V_{M\uparrow}=-2.0t$.

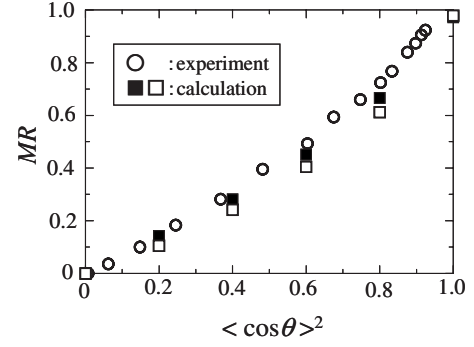


FIG. 6. Normalized values of MR, $[\rho(0) - \rho(H)]/\rho(0)$ as a function of $\langle \cos^2 \theta \rangle$. Closed and open squares are the calculated results for grains with $5 \times 5 \times 5^*$ and $8 \times 8 \times 8$, and circles show experimental values (Ref. 11).

those used in the previous simulations. The open squares in Fig. 4 are results using the previous parameter values $V_{M\downarrow} = V_{NM} = 0$ and $V_{M\uparrow} = -2.0t$. The concentration of magnetic atoms is fixed to be 20%. The results show that MR increases with decreasing grain size, showing the same tendency obtained before.²⁰ The MR ratio in this case, however, was estimated from the conductance for a finite system size, since the conductivity diverges for this choice of the parameter values in the \downarrow spin state. When the MR ratio is calculated from the resistivity, the value should be 1 independent of r . This means that the decrease in MR with increasing r shown by the open squares is caused by a finite size effect; the mean free path for \downarrow spin electrons is much longer than the system width.

We now compare these results to experimental results.^{13,14} Figure 5(b) shows the resistivity change $\Delta\rho = \rho(0) - \rho_p$ as a function of $1/r$. Both the calculated and experimental results show good linearity except for the smallest grain. The inset shows the resistivity change as a function of $\rho(0)$. We find that the calculated results reproduce the experimental tendency satisfactorily, though the magnitude is smaller in the calculated results than in the experimental results.

We have shown that $\Delta\rho$ in granular systems is well correlated with $1/r$, but the MR itself is not. Experiments, however, have reported that the MR is well scaled with $1/r$.¹³⁻¹⁵ The discrepancy may be explained by introducing a resistivity of host matrix which is independent of the grain size. Subject to existence of the resistivity, $\Delta\rho$ decreases, while the total resistivity tends to a constant value with increasing grain size,^{13,14} resulting in the decrease of the MR ratio with increasing grain size. The MR ratio calculated is rather independent of the concentration of magnetic atoms. A quantitative disagreement of the concentration and grain size dependence of MR ratio between the calculated and experimental results might be attributed to our neglect of the change in the distribution of magnetic atoms/grains in the annealing process.

It has been reported that the resistivity change as a function of H is well-scaled by $\langle \cos^2 \theta \rangle$,^{11,20} where θ is an angle between the directions of magnetization and H , and $\langle \dots \rangle$ indicates an average over θ . The result is also well reproduced in the present simulations, as shown in Fig. 6, and can be explained as follows. Let $\rho_{+(-)}$ be the resistivity of the

majority (minority) spin electrons scattered at the interface of a grain. When the magnetic moment of the grain makes an angle θ with the external magnetic field H , the up (down) spin resistivity in the global spin axis parallel to H is

$$\rho_{\uparrow(\downarrow)}(H) = \{\rho_+ + \rho_- + (-)\cos\theta(\rho_+ - \rho_-)\}/2. \quad (2)$$

Since the direction of the local magnetic moments of the grains is random, we average $\cos\theta$ over the distribution of θ and denote it as $\langle\cos\theta\rangle$. The total resistivity is

$$\rho(H) = \frac{1}{4} \left[\rho_+ + \rho_- - \langle\cos\theta\rangle^2 \frac{(\rho_+ - \rho_-)^2}{\rho_+ + \rho_-} \right], \quad (3)$$

and the MR ratio is proportional to $\langle\cos\theta\rangle^2$.

We have performed numerical simulations with a few specific parameter values of the random potential. The dependence of the MR ratio on the random potential have extensively been studied previously, and interpreted in terms of the so-called α parameter.^{2,3,9,25} Combining the results on the present geometrical effects on the GMR and dependence of the MR ratio on the parameter values studied previously, one may obtain a clear picture of the GMR in multilayers and granular systems.

We have neglected the effects of spin-flip scattering in this analysis. The spin-flip scattering may be strong in MGFs with low annealing temperature, in which isolated magnetic impurities remain. In these samples, the MR effect would not saturate with increasing H , and the simple two-current model fails to explain the GMR. We compared our results with experimental results wherein the GMR effect is clearly identified, as in magnetic multilayers. We expect that the spin-mixing conductance in such MGFs may be the same order of

magnitude as that in magnetic multilayers,²⁶ and will not alter the results at least qualitatively. The good linearity in both the calculated and experimental MRs shown in Fig. 6 indicates that the two-current model is a reasonable approximation for transport properties in magnetic multilayers and MGFs, including the anomalous Hall effect.²⁷

In conclusion, we have performed numerical simulations for the magnetoresistance of magnetic multilayers and granular films using a simple model, but with a larger system size than used before. The present results eliminate the incidental results caused by boundaries of the system and account for the experimental results. The present work showed that the resistivity change is proportional to the inverse of the grain size, in agreement with the experimental results. The decrease in MR ratio with increasing grain size could be explained by introducing a resistivity of the host matrix independent of the grain size. It is worth noting that the sufficiently large system size used in this work has made it possible to compare the calculated results with experimental ones. Since the simulation method used includes effects beyond the Born or mean field approximations, the present method may be useful to include realistic electronic structures when a high performance supercomputer is available. Some attempts along this line have already reported for multilayers and tunnel junctions.^{28–30}

This work was supported by a Grant-in-Aid for Scientific Research in Priority Area “Creation and control of spin current” from the Ministry of Education, Culture, Sports, Science and Technology (MEXT), Japan and Next Generation Super Computing Project, Nanoscience Program, MEXT, Japan.

*inoue@nuap.nagoya-u.ac.jp

¹P. Grünberg, R. Schreiber, Y. Pang, M. B. Brodsky, and H. Sowers, *Phys. Rev. Lett.* **57**, 2442 (1986).

²M. N. Baibich, J. M. Broto, A. Fert, F. Nguyen Van Dau, F. Petroff, P. Etienne, G. Creuzet, A. Friederich, and J. Chazelas, *Phys. Rev. Lett.* **61**, 2472 (1988).

³J. Inoue, A. Oguri, and S. Maekawa, *J. Phys. Soc. Jpn.* **60**, 376 (1991).

⁴P. M. Levy, in *Solid State Physics*, edited by H. Ehrenreich and D. Turnbull (Academic Press, San Diego, 1994), Vol. 47, p. 367.

⁵M. A. M. Gijs and G. E. W. Bauer, *Adv. Phys.* **46**, 285 (1997).

⁶E. Y. Tsymlal and D. G. Pettifor, *Solid State Physics* (Academic Press, New York, 2001), Vol. 56, p. 113.

⁷A. Fert, A. Barthelemy, and F. Petroff, in *Contemporary Concepts of Condensed Matter Science*, edited by D. L. Mills and J. A. C. Bland (Elsevier, Amsterdam, 2006), p. 153.

⁸J. Bass and W. P. Pratt, Jr., *J. Phys.: Condens. Matter* **19**, 183201 (2007).

⁹J. Inoue, in *Nanomagnetism and Spintronics*, edited by T. Shinjo (Elsevier, Amsterdam, 2009), p. 15.

¹⁰A. E. Berkowitz, J. R. Mitchell, M. J. Carey, A. P. Young, S. Zhang, F. E. Spada, F. T. Parker, A. Hutten, and G. Thomas, *Phys. Rev. Lett.* **68**, 3745 (1992).

¹¹J. Q. Xiao, J. S. Jiang, and C. L. Chien, *Phys. Rev. Lett.* **68**, 3749 (1992).

¹²J. Q. Xiao, J. S. Jiang, and C. L. Chien, *Phys. Rev. B* **46**, 9266 (1992).

¹³P. Xiong, G. Xiao, J. Q. Wang, J. Q. Xiao, J. S. Jiang, and C. L. Chien, *Phys. Rev. Lett.* **69**, 3220 (1992).

¹⁴J.-Q. Wang, P. Xiong, and G. Xiao, *Phys. Rev. B* **47**, 8341 (1993).

¹⁵T. A. Rabedeau, M. F. Toney, R. F. Marks, S. S. P. Parkin, R. F. C. Farrow, and G. R. Harp, *Phys. Rev. B* **48**, 16810 (1993).

¹⁶T. Valet and A. Fert, *Phys. Rev. B* **48**, 7099 (1993).

¹⁷P. A. Lee and D. S. Fisher, *Phys. Rev. Lett.* **47**, 882 (1981).

¹⁸G. E. W. Bauer, *Phys. Rev. Lett.* **69**, 1676 (1992).

¹⁹Y. Asano, A. Oguri, and S. Maekawa, *Phys. Rev. B* **48**, 6192 (1993).

²⁰Y. Asano, A. Oguri, J. Inoue, and S. Maekawa, *Phys. Rev. B* **49**, 12831 (1994).

²¹H. Itoh, J. Inoue, and S. Maekawa, *Phys. Rev. B* **51**, 342 (1995).

²²K. M. Schep, P. J. Kelly, and G. E. W. Bauer, *Phys. Rev. Lett.* **74**, 586 (1995).

²³P. Zahn, I. Mertig, M. Richter, and H. Eschrig, *Phys. Rev. Lett.* **75**, 2996 (1995).

²⁴T. N. Todorov, E. Yu Tsymlal, and D. G. Pettifor, *Phys. Rev. B*

- 54**, R12685 (1996).
- ²⁵I. A. Campbell and A. Fert, in *Ferromagnetic Materials*, edited by E. P. Wohlfarth (North-Holland, Amsterdam, 1982), Vol. 3, p. 747.
- ²⁶Q. Yang, P. Holody, S.-F. Lee, L. L. Henry, R. Loloee, P. A. Schroeder, W. P. Pratt, Jr., and J. Bass, Phys. Rev. Lett. **72**, 3274 (1994).
- ²⁷J. Inoue, T. Tanaka, and H. Kontani, Phys. Rev. B **80**, 020405(R) (2009).
- ²⁸E. Y. Tsybal, Phys. Rev. B **62**, R3608 (2000).
- ²⁹J. Kudrnovský, V. Drchal, C. Blaas, P. Weinberger, I. Turek, and P. Bruno, Phys. Rev. B **62**, 15084 (2000).
- ³⁰H. Itoh and J. Inoue, J. Magn. Soc. Jpn. **30**, 1 (2006).